


Simple model for mean stress in turbulent boundary layers

Praveen Kumar  and Krishnan Mahesh*

*Department of Aerospace Engineering and Mechanics, University of Minnesota,
Minneapolis, Minnesota 55455, USA*



(Received 4 November 2020; accepted 28 January 2021; published 10 February 2021)

The mean stress is one of the most important quantities of interest in turbulent boundary layers. The governing equations for the mean flow are used to derive a relation between the mean total stress and the mean velocity in a zero pressure gradient turbulent boundary layer, allowing the mean shear stress to be written as a function of wall-normal distance. The relation contains an unknown term, which is modeled using a linear function of the wall-normal distance, inspired by existing data sets. The model for the mean total stress requires the wall-normal mean velocity profile, which requires modeling if not available. The existing data sets and scaling arguments are used to obtain a simple and compact fit for the mean wall-normal velocity, which is subsequently used to obtain a simple model for the mean total stress. The model shows good agreement with the available simulation and experimental data for a large range of Reynolds number.

DOI: [10.1103/PhysRevFluids.6.024603](https://doi.org/10.1103/PhysRevFluids.6.024603)

I. INTRODUCTION

Flow over a solid surface or wall produces a thin region of high shear close to the wall due to no-slip condition at the surface imposed by viscosity. This thin near-wall region called the boundary layer has been one of the most studied fluid problems starting from the seminal work of Prandtl [1]. The high shear induces large tangential stresses at the wall, which leads to drag responsible for energy expenditure in aerodynamic and hydrodynamic applications. Under most practical conditions, the boundary layer is turbulent, which is often described using the first- and second-order flow field statistics since the instantaneous flow field is highly chaotic [2].

Wall shear stress is perhaps the most important quantity of interest in many wall-bounded flows, and is challenging to measure directly. Therefore, it is often obtained indirectly from the measured velocity profile. The Clauser chart is often used in zero pressure gradient (ZPG) turbulent boundary layers (TBLs) to obtain wall shear stress. However, Wei *et al.* [3] pointed out that the Clauser chart method can be problematic as it can potentially mask subtle Reynolds number (Re) dependent behavior. Even if the wall shear stress is obtained, it is really difficult to obtain the mean tangential or shear stress (called the total stress henceforth), which may be desirable, due to the fine resolution requirements near the wall to measure the velocity gradient accurately.

The total stress (T) has viscous and turbulent components; the former dominates only very close to the wall. As Re (the ratio of inertial to viscous forces) increases, the region of dominant viscous stress shrinks and almost all of the total stress in the TBL is the turbulent shear stress, also called the Reynolds shear stress [4]. The scaling and universality of turbulent mean flow and Reynolds stresses have been subjects of numerous studies in recent years [4,5]. Many common turbulent simulation techniques solve the time-averaged Navier-Stokes equations for the mean velocity, which requires

*kmahesh@umn.edu

a closure for the Reynolds shear stress term. The accuracy of these techniques relies heavily on the accuracy of the employed Reynolds stress model [6].

The shear stress in TBLs has been the subject of numerous past studies. Fukagata *et al.* [7] proposed a decomposition of skin friction into laminar, turbulent, and inhomogeneous parts using the momentum budget whereas Renard and Deck [8] used the mean kinetic energy budget to isolate the laminar and turbulent contribution to the skin friction. Hou *et al.* [9] proposed two methods of recovering the entire total stress profile from incomplete velocity data in TBLs. The first method used an exponential-polynomial curve fit, to recover the entire total stress profile using the data from the outer part of the boundary layer ($\eta = y/\delta > 0.3$, where δ is the boundary layer thickness). However, they found that the curve fit was sensitive to the quality of the data. Hence, they proposed a second method where a simple linear fit was used for the total stress in viscous units (denoted by the “+” superscript) weighted with $(1 - \eta)$, i.e., $(1 - \eta)T^+ = a\eta + b$. The value of $b \approx 1$ to satisfy the boundary condition and a was found to be independent of Re_θ , but loosely correlated with the shape factor H ($a \approx -H$). The linear fit showed good agreement with the data for $\eta < 0.4$ – 0.5 . They reported values of the model constants a and b from several experimental and simulation data sets, which showed significant scatter for a at high Re .

Mehdi and White [10] used the mean momentum balance to obtain an expression to evaluate the skin friction coefficient for TBLs. Their method requires the gradient of T which is difficult to evaluate directly from noisy shear stress profiles. To overcome this limitation, they fit a Whittaker smoother, using a small smoothing parameter, to the entire total stress profile, with the condition that the gradient of the fit always remains negative. They show this approach to be robust for experimental data with typical noisy shear stress profiles, for which there are limited ways to obtain skin friction. The present paper differs from their work in that our objective is to obtain a simple model for T valid for the entire boundary layer. The model for T will be obtained by first expressing T in terms of the velocity profile and then modeling the unknown term using physical insight and available databases.

The mean flow field in a TBL is two dimensional. However, the wall-normal velocity (V) is small, typically of the order $10^{-2}U$, and hence often not reported in literature. However, V is an important quantity which is directly related to the streamwise growth of the boundary layer thickness and it also relates to the entrainment of the inviscid outer flow to the boundary layer across the boundary layer edge. Wei and Klewicki [11] used the existing TBL data sets to show that V/V_e is independent of Re , where V_e is V at the boundary layer edge ($\eta = 1$).

The present paper proposes a simple model for T which is valid throughout the TBL at ZPG. The model is derived from the governing equations of the mean flow with the assumption of an equilibrium boundary layer. The model for T requires the wall-normal velocity (V) profile, which is seldom reported in literature. Hence, a simple and compact model for V in a ZPG TBL is also proposed in the process. The paper is organized as follows. Section II discusses the existing turbulent databases used in the present paper. The model is derived in Sec. III, followed by a discussion in Sec. IV. Section V concludes the paper.

II. TBL DATABASES

Table I lists the relevant details of all the simulation and experimental databases used in this paper. Note that the correlation $Re_\tau = 1.13 \times Re_\theta^{0.843}$ proposed by Schlatter and Örlü [12] is used to obtain Re_θ from the reported values of Re_τ in the experiments of Baidya *et al.* [15].

Figure 1 shows the profiles of T^+ and $-u'v'$ using the direct numerical simulation (DNS) data of Schlatter and Örlü [12]. It can be clearly observed that T^+ shows excellent collapse across all the data sets, whereas the collapse of $-u'v'$ is poor near the wall. This motivates modeling the total stress as opposed to only the $-u'v'$, which is a common practice in literature. Any such model for T^+ would be valid throughout the boundary layer and would be insensitive to Re . Figure 2 shows the profiles of V/V_e for a range of Re using the DNS data of [12]. The profiles show excellent collapse

TABLE I. TBL datasets considered in this paper.

Case	Re_θ	Re_τ	H	Database
S1000	1006	359	1.4499	DNS [12]
S2000	2001	671	1.4135	DNS [12]
S3030	3032	974	1.3977	DNS [12]
S4060	4061	1272	1.3870	DNS [12]
S5000	5000	1571	1.3730	DNS [13]
S6000	6000	1848	1.3669	DNS [13]
S6500	6500	1989	1.3633	DNS [13]
E13000	13000	4336	1.31	Expt. [14]
E31000	31000	10022	1.27	Expt. [14]
E21630	21632	5100	1.4135	Expt. [15]
E51520	51524	10600	1.4135	Expt. [15]

across a range of Re , showing that V/V_e is a function of η and independent of Re , as first observed by Wei and Klewicki [11].

III. MODEL DERIVATION

The boundary layer approximations for the time-averaged Navier-Stokes equations in Cartesian coordinates yield

$$\frac{\partial U}{\partial x} + \frac{\partial V}{\partial y} = 0, \quad (1)$$

$$U \frac{\partial U}{\partial x} + V \frac{\partial U}{\partial y} = -\frac{1}{\rho} \frac{dP}{dx} + \frac{\partial T}{\partial y} \quad (2)$$

where U and V are the streamwise (x) and the wall-normal (y) components of the mean velocity vector, ρ is the fluid density, P is the mean pressure, and T is the mean total stress, i.e., the sum of the viscous stress ($\nu \partial U / \partial y$) and the Reynolds shear stress ($-\overline{u'v'}$). ν is the kinematic viscosity.

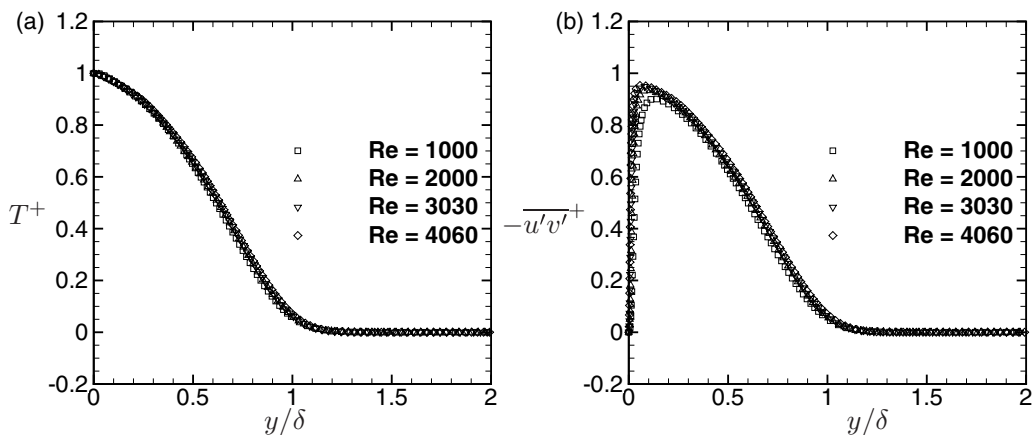


FIG. 1. Profiles of (a) T^+ and (b) $-\overline{u'v'}$ are shown in zero pressure gradient turbulent boundary layers using the DNS data of Schlatter and Örlü [12] (see Table I).

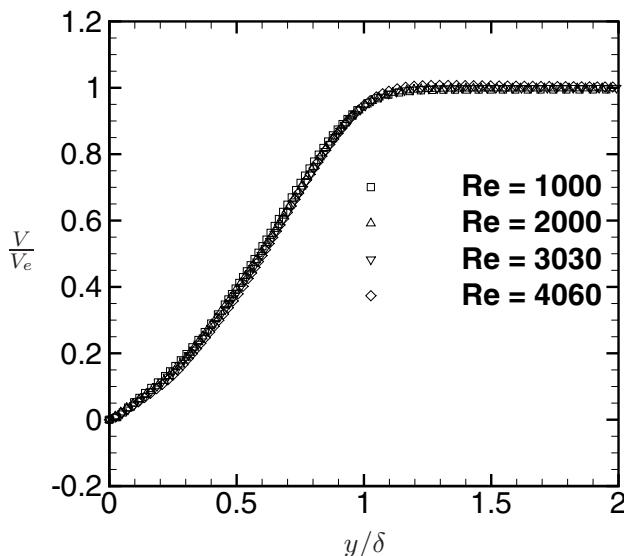


FIG. 2. Profiles of V/V_e are shown in zero pressure gradient turbulent boundary layers using the DNS data of Schlatter and Örlü [12] (see Table I).

Using Eqs. (1) and (2), it can be shown that

$$-U \frac{\partial V}{\partial y} - \left(y \frac{\partial U}{\partial y} + U_e \right) \frac{dU_e}{dx} = \frac{\partial T}{\partial y}. \quad (3)$$

Note that the subscript “e” denotes the edge of the boundary layer, the pressure gradient term in Eq. (2) is replaced by $U_e dU_e/dx$, and the approximation $V \approx -y dU_e/dx$ is used in Eq. (3). Now, the second term of Eq. (3) drops out for a zero pressure gradient boundary layer, yielding

$$-U_e \frac{\partial V}{\partial y} + F = \frac{\partial T}{\partial y}, \quad (4)$$

where $F = (U_e - U) \partial V / \partial y$. Integrating Eq. (4) from a generic y to $y = \delta$ yields

$$T = U_e V_e \left(1 - \frac{V}{V_e} \right) - \int_y^\delta F dy, \quad (5)$$

where δ is the boundary layer thickness often defined as the wall-normal distance where $U = 0.99U_e$. The friction velocity $u_\tau = \sqrt{\tau_w}/\rho$, where τ_w is the mean shear stress at the wall, is considered an appropriate inner velocity scale, in terms of which Eq. (5) becomes

$$T^+ = U_e^+ V_e^+ \left(1 - \frac{V}{V_e} \right) - \int_{y^+}^{\delta^+} F^+ dy^+. \quad (6)$$

Wei and Maciel [16] showed that $-\overline{u'v'}$ is of the order $U_e V_e$ at large Re. Hence, the last term of Eq. (6) (say I) is expected to be small. In fact, Kumar and Dey [17] showed that $-\overline{u'v'}$ varies linearly with $U_e V$ in the outer layer, which is equivalent to neglecting I and viscosity. In the present paper, such assumptions are avoided to obtain a model for the total stress valid for the entire turbulent boundary layer. Also, $U_e^+ V_e^+ = H$ for ZPG TBLs [11], where H is the shape factor (the ratio of the displacement thickness to the momentum thickness), which is a weak function of Re at large Re.

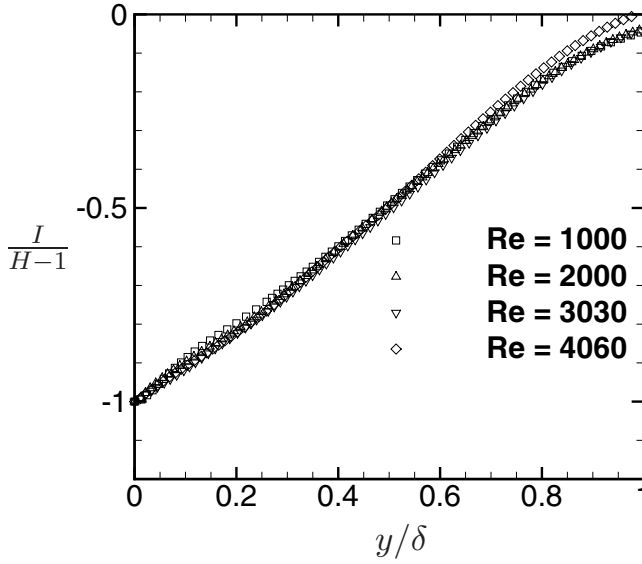


FIG. 3. $I/(H - 1)$ profiles are shown in zero pressure gradient turbulent boundary layers using the simulation data of Schlatter and Örlü [12].

Hence, it is expected that I is a weak function of Re . Also, by definition, I vanishes for $y/\delta \geq 1$. Using the data sets shown in Fig. 1, I can be obtained as

$$I = T^+ - U_e^+ V_e^+ \left(1 - \frac{V}{V_e}\right). \quad (7)$$

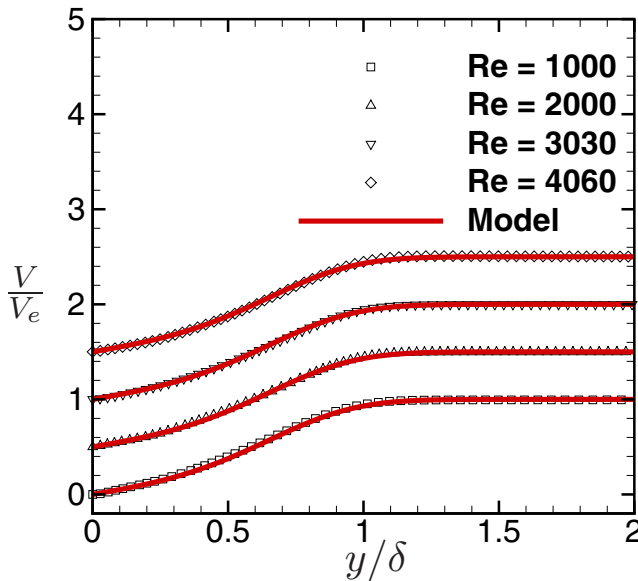


FIG. 4. The model for V/V_e is compared to the simulation data [12] (see Table I). Note that the profiles are shifted upwards by 0.5 for clarity.

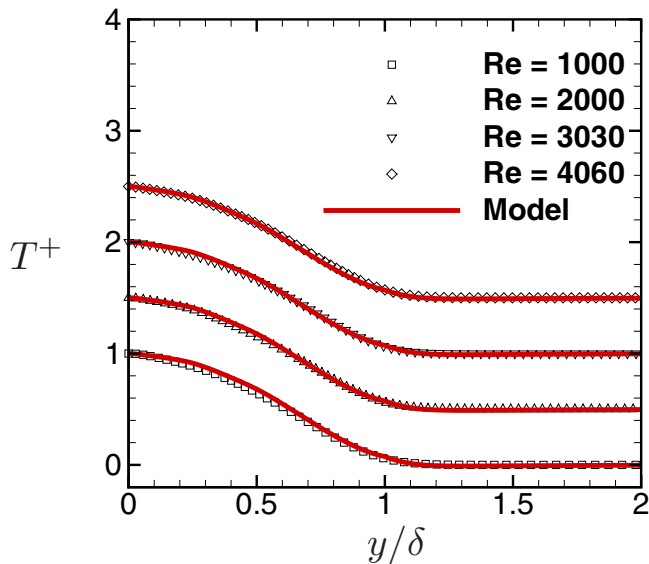


FIG. 5. The model for T^+ is compared to the simulation data [12] (see Table I). Note that the profiles are shifted upwards by 0.5 for clarity.

By using the definition of I and the self-similarity of TBL, it can be shown that $I(0) = (H - 1)/2$ (see Appendix A). Hence, it can be expected that $I/(H - 1)$ becomes insensitive to Re. Figure 3 shows $I/(H - 1)$ using the data sets of Fig. 1, showing a good collapse. Therefore, I is modeled as a simple linearly decreasing function of η to yield a modeled total stress

$$T^+ = H \left(1 - \frac{V}{V_e} \right) + (H - 1)(\eta - 1) \quad (8)$$

where the relation $H = U_e^+ V_e^+$ is used. Note that H has a small sensitivity to Re consistent with the earlier discussion about I .

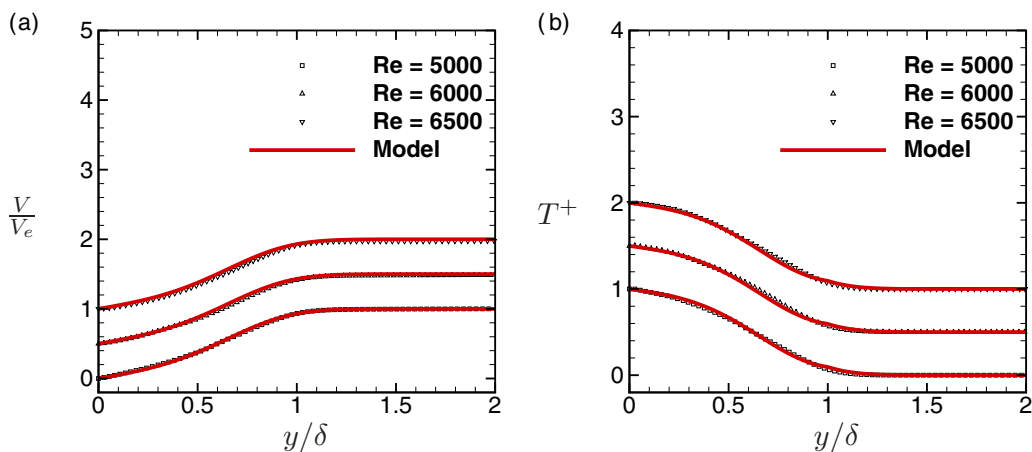


FIG. 6. Models for (a) V/V_e and (b) T^+ are compared to the simulation data at higher Re [13,18] (see Table I). Note that the profiles are shifted upwards by 0.5 for clarity.

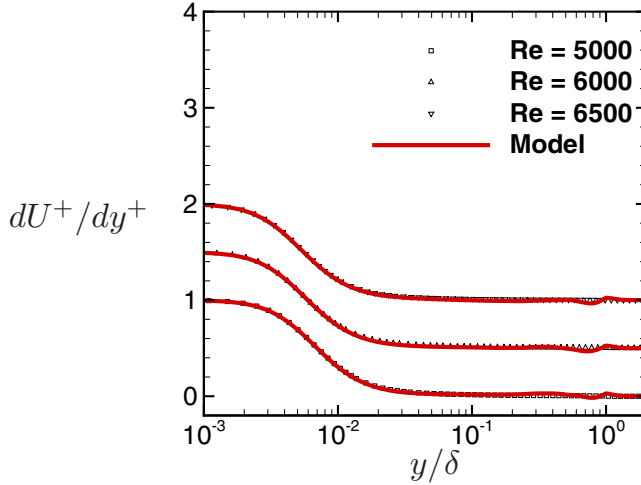


FIG. 7. The model for viscous stress (dU^+/dy^+) is compared to the simulation data [13,18] (see Table I). Note that the profiles are shifted upwards by 0.5 for clarity.

A major limitation of the derived model for T^+ [Eq. (8)] is that it presumes the availability of V , in the absence of which it requires a model for V . As shown in Sec. II, V/V_e is a function of η , increasing monotonically from zero at the wall to unity at $\eta = 1$ (Fig. 2). Hence, it is modeled using a hyperbolic tangent function as

$$\frac{V}{V_e} = \tanh(a\eta + b\eta^3). \quad (9)$$

It is found that the model constants $a = 0.5055$ and $b = 1.156$ give excellent fit with the data as shown in Fig. 4. The model is not too sensitive to the model constants (see Appendix B).

Equations (8) and (9) together yield a model for T^+ , i.e.,

$$T^+ = H \left(1 - \frac{V}{V_e} \right) + (H - 1)(\eta - 1). \quad (10)$$

Equation (10) can be written in terms of outer units as

$$\frac{T}{U_e V_e} = 1 - \frac{V}{V_e} + \left(\frac{H - 1}{H} \right) (\eta - 1). \quad (11)$$

Figure 5 shows the comparison of the modeled T^+ [Eq. (10)] with the data showing excellent agreement. Note that the models have used the DNS data shown in Fig. 1 to obtain model constants. Hence, the model performance is also tested for both V/V_e [Eq. (9)] and T^+ [Eq. (10)] models at higher Re [13,18] in Fig. 6 showing excellent agreement. As a more stringent test, modeled viscous stress (dU^+/dy^+) is obtained by subtracting the Reynolds shear stress from T^+ , and compared to the DNS data in Fig. 7 for the same datasets as Fig. 6. It is clear that the model performance is excellent throughout the boundary layer.

Next, the model for T^+ is tested at even higher Re using the experimental Reynolds shear stress data [14,15] in Fig. 8. There appear to be some discrepancies between the model predictions and the experimental data; however, the model still shows reasonable agreement.

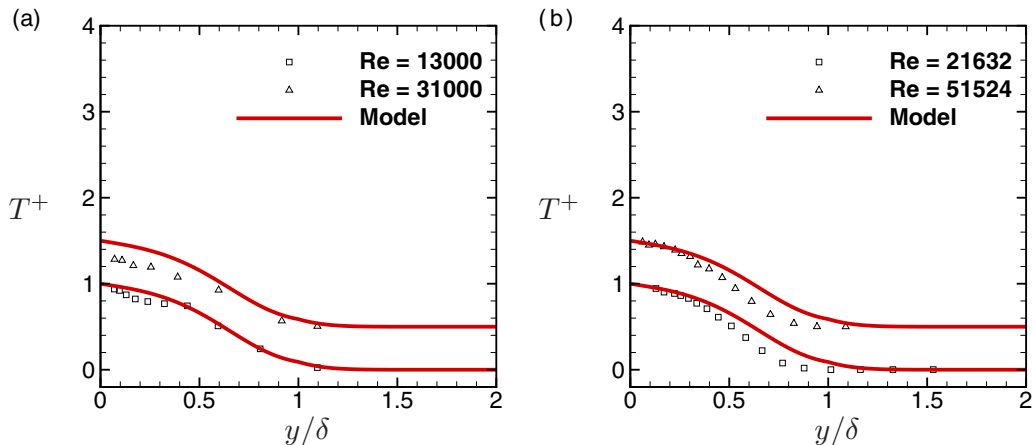


FIG. 8. The model for T^+ is compared to the Reynolds shear stress experimental data of (a) De Graaff and Eaton [14] and (b) Baidya *et al.* [15] (see Table I). Note that the profiles are shifted upwards by 0.5 for clarity.

IV. DISCUSSION

Multiplying both sides of Eq. (10) by $(1 - \eta)$, it can be shown that

$$(1 - \eta)T^+ = 1 - H\left(\frac{V}{V_e}\right) - \eta(2 - H) + H\eta\left(\frac{V}{V_e}\right) + (1 - H)\eta^2. \quad (12)$$

For small η , V/V_e is approximately linear in η , which makes the last two terms of Eq. (12) negligible. This explains why the fit proposed by Hou *et al.* [9] is a good approximation for small η and the slope of the linear fit is loosely related to H .

The apparent independence of the mean total stress with Re also suggests that it may be better to focus the modeling effort on the mean total stress rather than the Reynolds shear stress alone, if a universal model is desired. Nevertheless, the Reynolds shear stress contributes almost all of the mean total stress away from the wall. Hence, the model for the mean total stress can also be considered as a model for the Reynolds shear stress away from the wall.

V. CONCLUSION

The mean total stress profiles show very good collapse across a range of Re , motivating derivation of a model for the mean total stress. An expression is derived from the governing equations relating the mean total stress to the mean velocity, which involves a term I requiring modeling. The main assumption is that the flow satisfies the mean boundary layer equations with negligible pressure gradient. The term I is modeled using the available data by approximating $I/(H - 1)$ as a linear function of η .

The derived model requires a mean wall-normal velocity profile to obtain the mean total stress, which may not be available. Hence, the mean wall-normal velocity is also modeled using a simple compact function, assuming that the mean wall-normal velocity profile scaled with the edge wall-normal velocity becomes independent of Re . The model shows good performance for a large range of Re and, hence, is potentially useful for closure approaches like wall-modeled large eddy simulation. Complex flows have TBLs evolving under pressure gradients and transverse curvature. The present model requires extension to include such effects.

ACKNOWLEDGMENTS

This work is supported by ONR Grant No. N00014-20-1-2717. The authors thank Dr. P. Schlatter and Dr. J. Jiménez for making their simulation data available publicly [19,20].

 APPENDIX A: THE VALUE OF $I(0)$

The term I is a function of y which can be written as

$$I = - \int_y^\delta (U_e^+ - U^+) \frac{\partial V^+}{\partial y} dy = \int_y^\infty (U_e^+ - U^+) \frac{\partial U^+}{\partial x} dy = U_e^+ \int_y^\infty \frac{\partial U^+}{\partial x} dy - \frac{1}{2} \int_y^\infty \frac{\partial U^{+2}}{\partial x} dy. \quad (\text{A1})$$

Using the definition of displacement (δ^*) and momentum (θ) thicknesses, it can be shown that for a zero pressure gradient turbulent boundary layer

$$\int_0^\infty \frac{\partial U^+}{\partial x} dy = -U_e^+ \frac{\partial \delta^*}{\partial x}, \quad (\text{A2})$$

$$\int_0^\infty \frac{\partial U^{+2}}{\partial x} dy = -U_e^{+2} \left(\frac{\partial \delta^*}{\partial x} + \frac{\partial \theta}{\partial x} \right). \quad (\text{A3})$$

Using Eqs. (A2) and (A3) in Eq. (A1) after setting $y = 0$ yields

$$I(0) = \frac{1}{2} U_e^{+2} \left(\frac{\partial \delta^*}{\partial x} - \frac{\partial \theta}{\partial x} \right) = \frac{1}{2} U_e^{+2} \frac{\partial \theta}{\partial x} \left(\frac{\partial \delta^* / \partial x}{\partial \theta / \partial x} - 1 \right). \quad (\text{A4})$$

For a zero pressure gradient turbulent boundary layer, $U_e^{+2} d\theta/dx = 1$ and equilibrium implies $(d\delta^*/dx)/(d\theta/dx) = H$ [21]. Therefore, Eq. (A4) simplifies to

$$I(0) = \frac{1}{2}(H - 1). \quad (\text{A5})$$

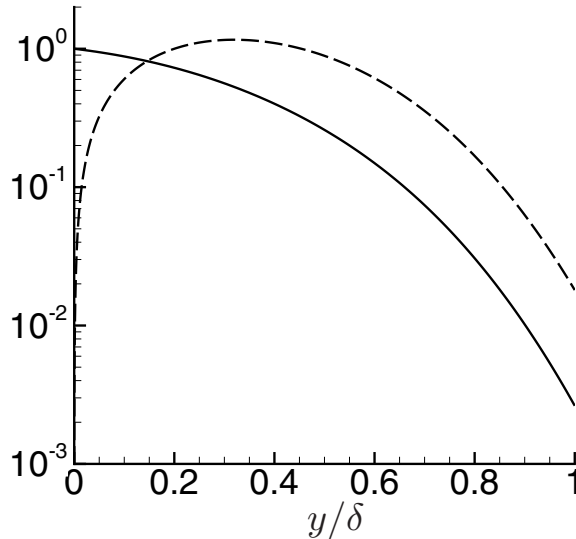


FIG. 9. Sensitivity of model constants for the V/V_e model: a (solid) and b (dashed).

APPENDIX B: SENSITIVITY TO MODEL CONSTANTS

The model for V is $V = V_e f$ where

$$f = \tanh\left[a\left(\frac{y}{\delta}\right) + b\left(\frac{y}{\delta}\right)^3\right]. \quad (\text{B1})$$

The function f has two model constants a and b . It can be shown that

$$\frac{\partial f}{\partial a} = \frac{y}{\delta}(1-f)^2, \quad (\text{B2})$$

$$\frac{\partial f}{\partial b} = 3\left(\frac{y}{\delta}\right)^2(1-f)^2. \quad (\text{B3})$$

Therefore, relative changes in f due to changes in the model constants, respectively, are

$$\frac{\Delta f}{f} = \left[a\left(\frac{y}{\delta}\right) \frac{(1-f)^2}{f} \right] \frac{\Delta a}{a}, \quad (\text{B4})$$

$$\frac{\Delta f}{f} = \left[3b\left(\frac{y}{\delta}\right)^2 \frac{(1-f)^2}{f} \right] \frac{\Delta b}{b}. \quad (\text{B5})$$

The terms in square brackets of Eqs. (B4) and (B5) are shown in Fig. 9. These terms represent relative change in f per unit relative to change in the model constants. It is clear that the sensitivity is small.

-
- [1] H. Schlichting, *Boundary-Layer Theory* (McGraw-Hill, New York, 1968).
 - [2] S. B. Pope, *Turbulent Flows* (Cambridge University, Cambridge, England, 2001).
 - [3] T. Wei, R. Schmidt, and P. McMurtry, Comment on the Clauser chart method for determining the friction velocity, *Exp. Fluids* **38**, 695 (2005).
 - [4] A. J. Smits, B. J. McKeon, and I. Marusic, High-Reynolds number wall turbulence, *Annu. Rev. Fluid Mech.* **43**, 353 (2011).
 - [5] I. Marusic, B. J. McKeon, P. A. Monkewitz, H. M. Nagib, A. J. Smits, and K. R. Sreenivasan, Wall-bounded turbulent flows at high Reynolds numbers: Recent advances and key issues, *Phys. Fluids* **22**, 065103 (2010).
 - [6] P. A. Durbin, Some recent developments in turbulence closure modeling, *Annu. Rev. Fluid Mech.* **50**, 77 (2018).
 - [7] K. Fukagata, K. Iwamoto, and N. Kasagi, Contribution of Reynolds stress distribution to the skin friction in wall-bounded flows, *Phys. Fluids* **14**, L73 (2002).
 - [8] N. Renard and S. Deck, A theoretical decomposition of mean skin friction generation into physical phenomena across the boundary layer, *J. Fluid Mech.* **790**, 339 (2016).
 - [9] Y. Hou, V. S. R. Somandepalli, and M. G. Mungal, A technique to determine total shear stress and polymer stress profiles in drag reduced boundary layer flows, *Exp. Fluids* **40**, 589 (2006).
 - [10] F. Mehdi and C. M. White, Integral form of the skin friction coefficient suitable for experimental data, *Exp. Fluids* **50**, 43 (2011).
 - [11] T. Wei and J. Klewicki, Scaling properties of the mean wall-normal velocity in zero-pressure-gradient boundary layers, *Phys. Rev. Fluids* **1**, 082401(R) (2016).
 - [12] P. Schlatter and R. Örlü, Assessment of direct numerical simulation data of turbulent boundary layers, *J. Fluid Mech.* **659**, 116 (2010).
 - [13] J. A. Sillero, J. Jiménez, and R. D. Moser, One-point statistics for turbulent wall-bounded flows at Reynolds numbers up to $\delta^+ \approx 2000$, *Phys. Fluids* **25**, 105102 (2013).
 - [14] D. B. De Graaff and J. K. Eaton, Reynolds-number scaling of the flat-plate turbulent boundary layer, *J. Fluid Mech.* **422**, 319 (2000).

- [15] R. Baidya, J. Philip, N. Hutchins, J. P. Monty, and I. Marusic, Distance-from-the-wall scaling of turbulent motions in wall-bounded flows, *Phys. Fluids* **29**, 020712 (2017).
- [16] T. Wei and Y. Maciel, Derivation of Zagarola-Smits scaling in zero-pressure-gradient turbulent boundary layers, *Phys. Rev. Fluids* **3**, 012601(R) (2018).
- [17] P. P. Kumar and J. Dey, Shape factor of the turbulent boundary layer on a flat plate and the Reynolds shear stress in the outer region, *Phys. Rev. Fluids* **4**, 024605 (2019).
- [18] M. P. Simens, J. Jiménez, S. Hoyas, and Y. Mizuno, A high-resolution code for turbulent boundary layers, *J. Comput. Phys.* **228**, 4218 (2009).
- [19] P. Schlatter, Boundary layer DNS/LES data, <https://www.mech.kth.se/~pschlatt/DATA/>.
- [20] J. Jiménez, DNS turbulent boundary layer data, <https://torroja.dmt.upm.es/ftp/blayers/>.
- [21] P. Kumar and K. Mahesh, Analysis of axisymmetric boundary layers, *J. Fluid Mech.* **849**, 927 (2018).